

# Intense Arctic Ozone Depletion in the Spring of 2011

JAMES W. HANNIGAN,<sup>1,2</sup> REBECCA L. BATCHELOR<sup>1</sup> and M.T. COFFEY<sup>1</sup>

(Received 2 September 2011; accepted in revised form 6 April 2012)

**ABSTRACT.** Observations of record-breaking ozone depletion during the Arctic spring of 2011 were made at 76° N in Thule, Greenland. The ozone total column amount of 290 DU measured on 18 March 2011 is the lowest value from the 12-year observation record and represents an ozone depletion of up to 48% of a typical March column. The unique 2010–11 vortex was characterized by sustained low stratospheric temperatures and stability that resisted breakup through March. Simultaneous observations of O<sub>3</sub>, HF, HCl, HNO<sub>3</sub>, and ClONO<sub>2</sub> demonstrate strong subsidence and substantial conversion of chlorine from its normal reservoirs.

**Key words:** Greenland, ozone, polar vortex, FTS, remote sensing

**RÉSUMÉ.** Au printemps 2011, des observations d'appauvrissement record de l'ozone ont été faites dans l'Arctique à 76° N à Thule, au Groenland. Le 18 mars 2011, la colonne d'ozone total a été mesurée à 290 DU, ce qui représente la valeur la plus faible depuis que les observations ont commencé à être consignées il y a 12 ans. Cela constitue un appauvrissement de l'ozone allant jusqu'à 48 % de la colonne typiquement enregistrée en mars. Le vortex unique dénoté en 2010-2011 était caractérisé par des températures stratosphériques faibles et soutenues ainsi que par une stabilité ayant résisté à la dissipation jusqu'en mars. Des observations simultanées de O<sub>3</sub>, HF, HCl, HNO<sub>3</sub> et ClONO<sub>2</sub> ont démontré une forte subsidence et une conversion substantielle du chlore à partir des réservoirs normaux.

**Mots clés :** Groenland, ozone, vortex circumpolaire, FTS, télédétection

Traduit pour la revue *Arctic* par Nicole Giguère.

## OBSERVATIONS

Since 1999, continuous observations have been made at high spectral resolution (0.0035 cm<sup>-1</sup>) of the infrared (750–4500 cm<sup>-1</sup>) absorption by the atmosphere from a site at Thule, Greenland (76.5° N, 68.7° W, 225 m asl) by a solar-viewing Fourier transform spectrometer (FTS). The observation program is operated as part of the Infrared Working Group (IRWG, <http://www.acd.ucar.edu/irwg>) of the Network for the Detection of Atmospheric Composition Change (NDACC, <http://www.ndacc.org>) (Kurylo, 1991; Kurylo and Zander, 2000). The network integrates chemical constituent and temperature measurements of the remote atmosphere from more than 80 sites around the globe that are instrumented with several types of remote sensing or balloon-borne sensors. Of these 80 sites, 17 are active FTS sites, four of which are in the Arctic. Vertical column amounts and low vertical resolution profiles are retrieved from the absorption spectra for a number of gases important to stratospheric ozone chemistry and to greenhouse warming effects (Hannigan et al., 2009). Measurements are archived as part of the NDACC and can be publicly accessed at [www.ndacc.org](http://www.ndacc.org).

Since the FTS is a solar viewing instrument, observations at Thule are discontinued each winter while the sun

is below the horizon, from approximately late October to late February. When measurements resume at each spring polar sunrise, we may or may not find the Arctic polar vortex to be in the vicinity of the Thule site, and often, the vortex will be in some stage of breaking apart. Consequently, the springtime evolution of gases involved in polar ozone depletion, chlorine reservoir species, and tracers will reveal some details about the later stages of the winter's polar ozone loss. These gases include ozone (O<sub>3</sub>), hydrogen chloride (HCl), chlorine nitrate (ClONO<sub>2</sub>), hydrogen fluoride (HF), and hydrogen nitrate (HNO<sub>3</sub>), which are among those routinely measured at the site. Other species important to polar chemistry, for instance ClO or the ClO dimer, have concentrations below the detection limit of the instrument.

Data presented here are computed from chemical volume mixing ratio (VMR) profile retrievals as discussed in Hannigan et al. (2009). The independent information in the profiles defined as the degrees of freedom for signal (DOFS) (Rodgers, 2000) ranges from 1 (ClONO<sub>2</sub>) to 4.5 (O<sub>3</sub>) and is between 2 and 3 for HCl, HF, and HNO<sub>3</sub>. Hence only total columns are reported for ClONO<sub>2</sub>. For the other gases, the retrieved profile information is in the 10–30 km region and higher to approximately 40 km for O<sub>3</sub>. There is little information from the troposphere for all gases shown here; the VMR plots (Figs. 1 and 2) show that the profiles tend to

<sup>1</sup> National Center for Atmospheric Research, Atmospheric Chemistry Division, PO Box 3000, Boulder, Colorado 80305, USA

<sup>2</sup> Corresponding author: [jamesw@ucar.edu](mailto:jamesw@ucar.edu)

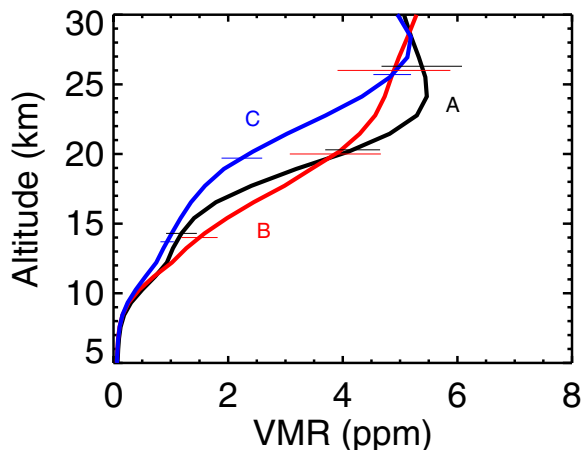


FIG. 1. Mean March ozone volume mixing ratios over Thule for the years 2000–10. Curve A (black) shows mean profiles of measurements made outside the vortex; Curve B (red) shows those inside the vortex; and Curve C (blue) shows the mean profile for 2011. Horizontal bars are the standard deviations of the profiles at three selected altitudes of 14, 20, and 26 km and are offset slightly for clarity.

return to the a priori state as sensitivity diminishes with altitude, which is expected in a well-behaved retrieval. To estimate the losses given in Tables 1 and 2 and the text, whether caused by chemical reaction, activation from reservoir species, or condensation from the gas phase, we use partial and total column amounts. To calculate these abundances, we used the same a priori temperature and pressure data from the National Centers for Environmental Prediction (NCEP) that were used for the retrievals and in Figure 3.

The focus of this paper is to illustrate and analyze the large stratospheric  $O_3$  loss in 2011 by contrasting the 2011 measurements with those taken at the same site and in the same time interval in the preceding 11 years. This paper highlights the importance of the long duration, fixed-station, and multi-species dataset. Measurements in some years started as early as 20 February, but typically began in the first week of March. In 2011, measurements ceased on 19 March; therefore, the datasets for each species from the previous years are limited to no later than 19 March. Moreover the previous year's daily observations are binned as inside or outside the polar vortex. For 2011, all measurements are inside the vortex.

## DISCUSSION

Figure 1 shows the mean ozone VMR vertical profile for three conditions at Thule in March. Curve A (black) is the average of profiles from 11 years (2000–10) of observations outside the outer edge of the Arctic polar vortex, and curve B (red) is the average over the same time period of observations made inside the inner edge. The outer and inner boundaries of the polar vortex are defined here as the regions outside and inside the potential vorticity contour of  $2.0 \times 10^{-5}$  ( $2.5 \times 10^{-5}$ )  $\text{km}^2\text{kg}^{-1}\text{s}^{-1}$  on the 440 K potential temperature surface (Coffey et al., 1999, 2008; Feng et al.,

2005). To illustrate the inside/outside contrast, the observations in the collar region between  $2.0$  and  $2.5 \times 10^{-5}$   $\text{km}^2\text{kg}^{-1}\text{s}^{-1}$  have been excluded. Curve A is the average of 102 profiles from 50 days in March, and curve B is the average of 34 profiles from the 21 days when measurements were made within the polar vortex. Curve C (blue) is the average profile for March 2011 (7 days, 13 profiles), when all measurements were inside the vortex (PV at 440 K ranged from  $3.5$  to  $3.77 \times 10^{-5}$   $\text{km}^2\text{kg}^{-1}\text{s}^{-1}$ ; previous high PV was  $3.35 \times 10^{-5}$  in 2007). The thin horizontal bars are the standard deviations (SD) of the profiles at three selected levels of 14, 20, and 26 km (offset vertically for clarity) to illustrate the variability in the data. These three profile types presenting data from separate time regimes with three SD bars are used in all subsequent plots of gases and temperatures.

Curve C, when integrated, yields the lowest average total column ozone observed in the vortex at Thule in March since observations began in 1999, corresponding to a mean total column of 309 Dobson units (DU) (Table 1). This mean total includes the minimum value from the 12-year observation record of 290 DU, measured on 18 March 2011, which represents an ozone depletion of up to 48% of a typical March column. The mean total  $O_3$  for March in 2000–10 is 445 and 448 DU inside and outside the vortex respectively (Table 1). These values are controlled not only by chemical loss, but also by large-scale poleward and downward transport (e.g., WMO, 2006). The buildup of  $O_3$  over the winter causes the March averages to be the highest values of the year. Ozone profiles are highly variable, both year to year, as shown by the large and overlapping standard deviation bars on curves A and B in Figure 1, and on much shorter time scales, because of tropopause height variability, mixing, and transport (Hood et al., 2001; Salby and Callaghan, 2007). Yet when accounting for descent using a passive tracer method as described below (Table 2), we estimate that in 2011, 45% of the ozone total column was depleted compared to the average March total column from the previous 11 years. Curve C shows extended chemical depletion of ozone from approximately 15 to 25 km and diminishing loss to 28 km relative to the outside vortex distribution (Curve A). In contrast, the mean from other March observations in the vortex (Curve B) shows a modest ozone loss between 19 and 28 km, indicative (but not conclusively) of active destruction of ozone. The higher  $O_3$  level in the 12 and 19 km region shown in Curve B in contrast to Curve A may be due to descended ozone-rich air that has not been chemically depleted. Curve A is likely influenced more strongly by horizontal mixing of lower latitude air (WMO, 2006).

The year 2011 was a persistently cold one in the Arctic (Manny et al., 2011). Figure 3 shows March NCEP analysis temperatures (Finger et al., 1993) at Thule for the same dates on which observations were made in the 2000–11 time period. Cold temperatures (less than  $T_{\text{act}} \sim 196$  K) enable the formation of polar stratospheric clouds (PSCs) that can sequester gaseous  $\text{HNO}_3$  and on which the primary stratospheric chlorine reservoir species  $\text{HCl}$  and  $\text{ClONO}_2$

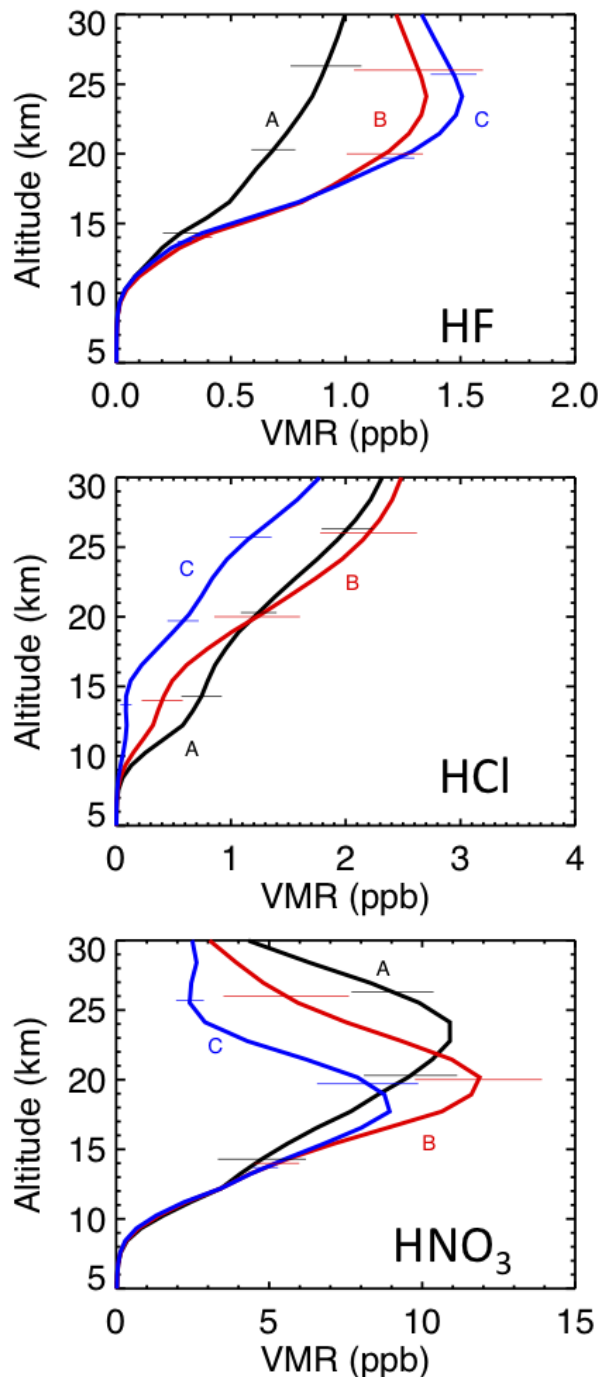


FIG. 2. Volume mixing ratio profiles for HF (top), HCl (middle) and  $\text{HNO}_3$  (bottom). Curve details as in Figure 1.

can react, releasing activated chlorine that can catalytically destroy ozone (Webster et al., 1993; Drdla et al., 2002). While PSCs often form to various extents during Arctic winters, the persistence of sufficiently low temperatures over a wide altitude range was unique in 2011 (Manney et al., 2011), ultimately leading to the large  $\text{O}_3$  loss (Harris et al., 2010). Over Thule, the effect of the atypically cold temperatures up to 27 km that were seen on observation days, in combination with the effects of PSCs and activated Cl, led to unusual  $\text{O}_3$  loss in March 2011.

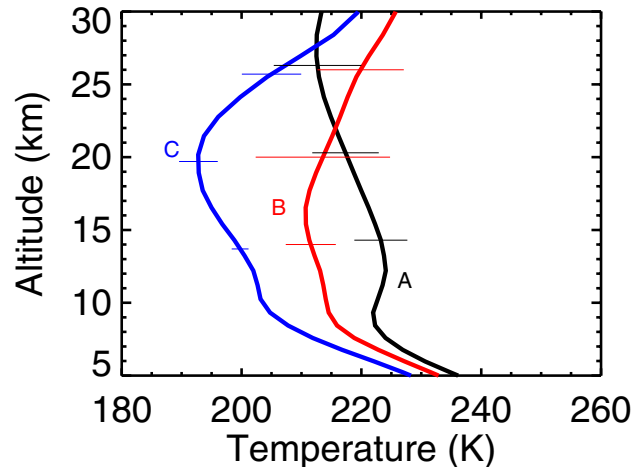


FIG. 3. Mean temperature profiles from those observation days included in the trace gas figures. Curve details as in Figure 1. Temperature profiles are from the National Centers for Environmental Prediction.

The top panel of Figure 2 shows the HF VMR profile for the three conditions as described above. HF has a long chemical lifetime in the stratosphere and can be used as a passive tracer of vortex dynamics (Chipperfield et al., 1997; Coffey et al., 2003) because its mixing ratio profile increases sharply with altitude above the tropopause. The elevated levels in the middle stratosphere of the 2011 HF profile (Curve C) are consistent with strong descent within the vortex. We estimate this descent to be at least 2 km/month at 30 km, similar to the descent found by Abrams et al. (1996) in the Arctic vortex in 1992–93. The SD bars on Curve A show the low variability outside the vortex, while Curve B shows considerable variability due only to dynamics. Curve C shows the highest values above 18 km indicative of the persistent vortex and the differential rate of descent with altitude (WMO, 2003). Using HF as a tracer of dynamical subsidence in the vortex, one can estimate the amount of chemical removal of several species. Descent is accounted for by comparing the ratio of the quantity (partial or total column) to HF and the ratio of the March mean from all years for that quantity to HF. Table 2 shows results of March 2011 conditions for the total column and three partial column layers of 9–16, 16–23, and 23–30 km calculated using this method. Ozone loss is 32% in the 9–16 km layer; 60% in the 16–23 km layer, where the volume of PSCs was highest; and 38% up to 30 km.

Figure 2 also shows VMR profiles of HCl (middle panel) and  $\text{HNO}_3$  (bottom panel) for the same three conditions as in Figure 1. Curve B for HCl shows loss of HCl in the 12–18 km region inside the vortex in March of past years. In contrast, nearly all of the HCl is removed in the 10–15 km altitude range in March 2011. As shown in Table 2, this HCl depletion is as high as 84% in the 9–16 km partial column and 73% in the 16–23 km range. This nearly complete activation of HCl is similar to observations from Esrange early in the 2002–03 winter reported in a case study by Feng et al. (2005). In the same study, extremely low temperatures above the potential temperature of 672 K

TABLE 1. Mean total column densities (Dobson units for O<sub>3</sub>, molecules/cm<sup>2</sup> all others) of each gas during March for measurements outside the vortex, inside the vortex for all previous March data (boundaries as defined in the text) and during 2011 over Thule.

Region	O <sub>3</sub>	HNO <sub>3</sub>	HF	HCl	ClONO <sub>2</sub>
Extra-vortex	448	2.81e + 16	2.05e + 15	4.88e + 15	1.64e + 15
In-vortex	445	2.94e + 16	2.90e + 15	3.86e + 15	3.56e + 15
2011	309	2.30e + 16	2.73e + 15	1.76e + 15	2.31e + 15

TABLE 2. Percentage depletion in individual layers and total column. This value is calculated as the percent difference between two ratios: the ratio of the column of the gas of interest to HF in March 2011 and the mean ratio of that column to HF over all other years. The column labeled HF shows the percent difference between the March 2011 column and the March mean for 2000–10.

Column	O <sub>3</sub>	HNO <sub>3</sub>	HF	HCl	ClONO <sub>2</sub>	HCl + ClONO <sub>2</sub>
09–16 km	32.4	8.3	-13.1	84.7		
16–23 km	60.2	46.2	-43.6	73.2		
23–30 km	38.7	78.7	-14.2	58.8		
Total	45.4	34.7	-25.0	70.8	6.8	51.8

(approximately 26 km) and consequent O<sub>3</sub> loss were seen in late March. Here, we find low mixing ratios of HCl at higher altitudes, with a loss of 58% in the 23–30 km partial column. There is evidence for Cl activation, though this finding is inconclusive at higher altitudes in the range as the sensitivity of the measurement diminishes towards 30 km and above. When combining this information with ClONO<sub>2</sub> measurements, we find that 51% of the chlorine in the total column is unaccounted for by these primary reservoir species. Given that temperatures are sufficiently low for continued PSC formation and chlorine activation, this chlorine is likely still in active forms.

Nitric acid profiles (Fig. 2) highlight subsidence of air inside the vortex (as also seen in the HF profile) and a large depletion in the peak distribution of HNO<sub>3</sub> near 25 km in 2011. This depletion represents approximately 46% of the 16–23 km partial column, 78% of the 23–30 km partial column, and 34% of the total column relative to previous years (Table 2). This depletion could be due to three causes: 1) the condensation of HNO<sub>3</sub> into PSC particles; 2) sedimentation of the growing particles, which removes HNO<sub>3</sub> from the stratosphere to the troposphere; and 3) competition in the stratosphere for NO<sub>2</sub>, the main source of HNO<sub>3</sub>, which by now is more abundant than ClO (Coffey et al., 2003). From Table 1, the March extra-vortex ClONO<sub>2</sub> total column from all previous years is lower than previous in-vortex and March 2011 means. The in-vortex total column mean is more than twice the extra-vortex mean, representing some conversion from active Cl via its more typical pathway in the Arctic to ClONO<sub>2</sub> reservoir (Santee et al., 1996). In 2011, though the column is only 6% lower than all previous March values (Table 2), it is 64% of the previous in-vortex mean column and is further evidence for persistent activated Cl and subsequent chemical destruction of ozone. The low HNO<sub>3</sub> illustrated in Curve C and Tables 1 and 2 and the delay of recovery of the ClONO<sub>2</sub> reservoir depict a polar spring scenario for 2011 that is more like the Antarctic than the Arctic (Manney, 2011). Up to the time measurements ceased, we could see no evidence of HNO<sub>3</sub>

returned to the gas phase after possible sedimentation. This finding may be due to the lack of the retrieval's sensitivity and vertical resolution in the retrieved profiles, or it may mean that sedimented HNO<sub>3</sub> has not yet evaporated back to the gas phase. We also have no evidence of low NO<sub>2</sub> levels that would limit HNO<sub>3</sub> formation.

## CONCLUSIONS

Observations from Arctic sunrise through 19 March made at the NDACC site in Thule, Greenland, over the 12-year span 2000–11 indicate that the 2011 Arctic spring-time stands out as exceptionally cold, characterized by substantial ozone loss of up to 45% of the mean total column relative to the previous 10 years. Consistent with this ozone depletion and ongoing cold temperatures, we observe substantial loss of HCl throughout the stratosphere and low total column of ClONO<sub>2</sub> through March, which prolongs activated Cl and thus contributes to the large O<sub>3</sub> loss. The observations of HNO<sub>3</sub> showed loss that removed nitrogen, which in a more typical year would be integral to deactivating Cl by producing ClONO<sub>2</sub>. Relative chemical loss was estimated using the passive tracer HF, which showed a marked redistribution downward of the HF VMR profile indicating very active descent within the vortex.

## ACKNOWLEDGEMENTS

The National Center for Atmospheric Research is supported by the National Science Foundation. The NCAR FTS observation program at Thule, Greenland, is supported under contract by the National Aeronautics and Space Administration. This work also is supported by the NSF Office of Polar Programs. We wish to thank the Danish Meteorological Institute for support at the Thule site.



## REFERENCES

- Abrams, M.C., Manney, G.L., Gunson, M.R., Abbas, M.M., Chang, A.Y., Goldman, A., Irion, F.W., et al. 1996. Trace gas transport in the Arctic vortex inferred from ATMOS ATLAS-2 observations during April 1993. *Geophysical Research Letters* 23(17):2345–2348.
- Chipperfield, M.P., Burton, M., Bell, W., Paton Walsh, C., Blumenstock, T., Coffey, M.T., Hannigan, J.W., et al. 1997. On the use of HF as a reference for the comparison of stratospheric observations and models. *Journal of Geophysical Research* 102(D11):12901–12919.
- Coffey, M.T., Mankin W.G., and Hannigan, J.W. 1999. A reconstructed view of polar stratospheric chemistry. *Journal of Geophysical Research* 104(D7):8295–8316.
- Coffey, M.T., Mankin, W.G., Hannigan, J.W., and Toon, G.C. 2003. Airborne spectroscopic observations of chlorine activation and denitrification of the 1999/2000 winter Arctic stratosphere during SOLVE. *Journal of Geophysical Research* 107, 8303, doi:10.1029/2001JD001085.
- Coffey, M.T., Hannigan, J.W., Goldman, A., Kinnison, D., Gille, J.C., Barnett, J.J., Froidevaux, L., et al. 2008. Airborne Fourier transform spectrometer observations in support of EOS Aura validation. *Journal of Geophysical Research* 113, D16S42, doi:10.1029/2007JD008833.
- Drda, K., Gandrud, B.W., Baumgardner, D., Wilson, J.C., Bui, T.P., Hurst, D., Schauffler, S.M., Jost, H., Greenblatt, J.B., and Webster, C.R. 2002. Evidence for the widespread presence of liquid-phase particles during the 1999–2000 Arctic winter. *Journal of Geophysical Research* 107, 8318, doi:10.1029/2001JD001127.
- Feng, W., Chipperfield, M.P., Davies, S., Sen, B., Toon, G., Blavier, J.F., Webster, C.R., et al. 2005. Three-dimensional model study of the Arctic ozone loss in 2002/2003 and comparison with 1999/2000 and 2003/2004. *Atmospheric Chemistry and Physics* 5:139–152.
- Finger, F.G., Gelman, M.E., Wild, J.D., Chanin, M.L., Hauchecorne, A., and Miller, A.J. 1993. Evaluation of NMC upper-stratospheric temperature analyses using Rocketsonde and Lidar data. *Bulletin of the American Meteorological Society* 74(5):789–799.
- Hannigan, J.W., Coffey, M.T., and Goldman, A. 2009. Semi-autonomous FTS observation system for remote sensing of stratospheric and tropospheric gases. *Journal of Atmospheric and Oceanic Technology* 26:1814–1828, doi:10.1175/2009JTECHA1230.1.
- Harris, N.R.P., Lehmann, R., Rex, M., and von der Gathen, P. 2010. A closer look at Arctic ozone loss and polar stratospheric clouds. *Atmospheric Chemistry and Physics* 10:8499–8510, doi:10.5194/acp-10-8499-2010.
- Hood, L.L., Soukharev, B.E., Fromm, M., and McCormack, J.P. 2001. Origin of extreme ozone minima at middle to high northern latitudes. *Journal of Geophysical Research* 106(D18):20925–20940.
- Kurylo, M.J. 1991. Network for the detection of stratospheric change. *Proceedings of the Society of Photo-Optical Instrumentation Engineers* 1491:168–174, <http://dx.doi.org/10.1117/12.46658>.
- Kurylo, M.J., and Zander, R. 2000. The NDSC—its status after 10 years of operation. *Proceedings of the 19th Quadrennial Ozone Symposium, Hokkaido University Sapporo, Japan.* 167–168.
- Manney, G.L., Santee, M.L., Rex, M., Livesey, N.J., Pitts, M.C., Veefkind, P., Nash, E.R., et al. 2011. Unprecedented Arctic ozone loss in 2011. *Nature* 478:469–475, doi:10.1038/nature10556.
- Rodgers, C.D. 2000. *Inverse methods for atmospheric sounding: Theory and practice.* Singapore: World Scientific Publishing Co.
- Salby, M.L., and Callaghan, P.F. 2007. On the wintertime increase of Arctic ozone: Relationship to changes of the polar-night vortex. *Journal of Geophysical Research*, 112, D06116, doi:10.1029/2006JD007948.
- Santee, M.L., Froidevaux, L., Manney, G.L., Read, W.G., Waters, J.W., Chipperfield, M.P., Roche, A.E., Kumer, J.B., Mergenthaler, J.L., and Russell, J.M., III. 1996. Chlorine deactivation in the lower stratospheric polar regions during late winter: Results from UARS. *Journal of Geophysical Research* 101(D13):18835–18859, doi:10.1029/96JD00580.
- Webster, C.R., May, R.D., Toohey, D.W., Avallone, L.M., Anderson, J.G., Newman, P., Lait, L., Schoeberl, M.R., Elkins, J.W., and Chan, K.R. 1993. Chlorine chemistry on polar stratospheric cloud particles in the Arctic winter. *Science* 261(5125):1130–1133.
- WMO (World Meteorological Organization). 2003. *Scientific assessment of ozone depletion: 2002.* Global Ozone Research and Monitoring Project—Report No. 47. Geneva, Switzerland: WMO. 498 p.
- . 2007. *Scientific assessment of ozone depletion: 2006.* Global Ozone Research and Monitoring Project—Report No. 50. Geneva, Switzerland: WMO.